

Cite this: *J. Mater. Chem. A*, 2019, 7, 14613

Facile and mild preparation of brookite-rutile heterophase-junction TiO₂ with high photocatalytic activity based on a deep eutectic solvent (DES)[†]

Qian Wang,[‡] Huaiyan Ren,[‡] Yingqiang Zhao, Xinyuan Xia, Fang Huang, Guanwei Cui, Bohui Dong and Bo Tang^{‡*}

The phase junction of nano-TiO₂ plays an important role in enhancing its photocatalytic activity. However, the achievement of the green, mild and controllable synthesis of phase-junction nano-TiO₂ still remains a big challenge for the large-scale preparation and application. Deep eutectic solvents (DESs) show many advantages in the green and mild preparation of highly active nanomaterials due to their low cost, high environmental friendliness, easy large-scale preparation, tailored structures and tunable properties. In this study, by sharing two H-bond acceptors with one H-bond donor, we successfully used DES as a solvent, template, inhibitor and crystalline phase control agent simultaneously to controllably synthesize heterophase-junction nano-TiO₂ with different phase ratios under green and mild reaction conditions (at 180 °C for 18 h). The H₂ production rate of photocatalytic water splitting with this catalyst reached up to 14.51 mmol h⁻¹ g⁻¹, which was 20-fold greater than that of commercial P25 TiO₂ and also much higher than those of other TiO₂ nanostructures. To the best of our knowledge, this rate is the highest value reported so far for photocatalytic H₂ production catalyzed by sole TiO₂. This higher activity was mainly attributed to the phase junctions and defects. This study will provide a new way for the green, mild, easily controllable and versatile preparation of phase-junction photocatalysts with high efficiency.

Received 7th March 2019
Accepted 13th May 2019

DOI: 10.1039/c9ta02500f

rsc.li/materials-a

1. Introduction

TiO₂ is one of the most promising photocatalysts due to its excellent properties such as nontoxicity, low cost, excellent chemical stability and photocorrosion resistance.¹ However, the easy recombination of photogenerated electrons and holes of single-phase TiO₂ results in its lower photocatalytic activity.² Thus, many researchers have focused on how to effectively separate the photogenerated electron-hole pairs. It has been confirmed that the fabrication of heterophase junctions is an effective strategy for achieving the efficient separation and transfer of photogenerated electron-hole pairs.³ At present, numerous phase-junction TiO₂ samples such as anatase/rutile,^{3,4} anatase/brookite,⁵ brookite/rutile,⁶ and anatase/rutile/

brookite⁷ have been successfully prepared, dramatically enhancing the photocatalytic activity. However, some issues need to be solved in the phase-junction preparation process of nanomaterials; these include complicated reaction system, multi-step synthesis, addition of an acid or alkali (such as hydrochloric acid, glacial acetic acid, sodium hydroxide or ammonia), higher calcination temperatures and difficult tunability of two-phase or three-phase ratios, which lead to poor repeatability, low environmental friendliness and high energy consumption of the phase-junction TiO₂ preparation process. These issues have severely hindered the large-scale preparation and application of nanomaterials. Therefore, the development of facile, green and mild methods for tunable phase-junction TiO₂ is still highly desired.

Deep eutectic solvents (DESs), as advanced neoteric ionic solvents, have some additional advantages besides similar physical and chemical properties to those of conventional ionic liquids, such as facile preparation, low cost, high environmental friendliness and high atom economy.⁸ Moreover, their physicochemical properties can be easily tailored by changing the types of hydrogen-bond donors and hydrogen-bond acceptors as well as the flexible and adjustable raw material ratios. It has been proven that DESs are promising to replace organic

College of Chemistry, Chemical Engineering and Materials Science, Collaborative Innovation Center of Functionalized Probes for Chemical Imaging in Universities of Shandong, Key Laboratory of Molecular and Nano Probes, Ministry of Education, Shandong Provincial Key Laboratory of Clean Production of Fine Chemicals, Shandong Normal University, Jinan, Shandong, 250014, PR China. E-mail: wangqian@sdu.edu.cn; tangb@sdu.edu.cn

[†] Electronic supplementary information (ESI) available. See DOI: 10.1039/c9ta02500f

[‡] These authors contributed equally.

solvents and templates in the preparation of shape-controlled nanomaterials with higher catalytic activity under mild conditions. For example, Gutierrez and co-workers⁹ prepared hierarchical porous multiwalled CNT composites with high surface areas and outstanding conductivities by using ChCl/ethylene glycol (EG) DES as the template. Our previous work also demonstrated that DESs can be used for the green, mild, fast and controllable preparation of nanomaterials as solvents, template agents and inhibitors at the same time.¹⁰ However, until now, there are very few reports about the use of DESs in nanomaterial synthesis, especially in the fabrication of heterophase junctions. As far as we know, the green, mild and facile preparation of TiO₂ heterophase junctions by using DES as the solvent, template, inhibitor and crystalline phase control agent at the same time has not yet been reported. In our previous study, we found that the H-bond acceptors not only changed the morphologies of nano-TiO₂, but also changed its crystalline phases. Therefore, we deduced that a heterophase junction should be prepared using the designed DES by sharing two H-bond acceptors with one H-bond donor.

In this work, ChCl/betaine/oxalic acid DES was prepared and used for the facile synthesis of phase-junction TiO₂ under mild reaction conditions as the solvent, template, inhibitor and crystalline phase control agent. Then, the photocatalytic activity for water splitting into hydrogen was investigated. Finally, the cause of high photocatalytic activity was explored. These findings will provide a new method for the green, mild and easily controllable preparation of phase-junction catalysts with high activity; they will also provide a new way for the batch preparation of nanocatalysts at the same time due to the facile synthesis process, mild synthesis conditions and the advantages of DESs, such as high environmental friendliness, low cost, easy large-scale preparation and low vapor pressure.

2. Experimental section

2.1. Materials

Tetrabutyl titanate (TBOT, $\geq 99\%$ purity) was purchased from Shanghai Aladdin Biochemical Technology Co., Ltd, China. The commercial P25 TiO₂ was supplied from Beijing Entrepreneur Science & Trading Co., Ltd, China. ChCl, betaine, oxalic acid, methyl alcohol, and ethyl alcohol were obtained from Sino-pharm Chemical Reagent Beijing Co., Ltd, China.

2.2. DES preparation

DESs were synthesized by mixing hydrogen-bond acceptors ChCl and betaine with hydrogen-bond donor oxalic acid with a molar ratio of acceptor to donor of 1 : 1 at 70 °C for 2–3 h until clear, transparent, homogeneous target liquids appeared. In addition, the molar ratios of two hydrogen-bond acceptors (ChCl and betaine) were changed from 1 : 6 to 6 : 1.

2.3. TiO₂ preparation

First, 1 mL TBOT was added dropwise into the solvent mixture containing 15.5 mL ChCl/betaine/oxalic acid DES and 0.5 mL distilled water under vigorous stirring. Then, the obtained

mixture was transferred into a 25 mL Teflon-lined stainless steel autoclave. The autoclave was put into an oven and heated at 180 °C for 18 h. After naturally cooling down to room temperature, the white precipitate was harvested *via* centrifugation, washed thoroughly with absolute ethanol and distilled water, and dried at 60 °C for 5 h.

2.4. Hydrogen evolution test

The photocatalytic H₂ evolution experiments were carried out in a 20 mL quartz vessel sealed with a silicone rubber septum at an ambient temperature under atmospheric pressure. First, 1 mg as-prepared phase-junction TiO₂ was suspended in 10 mL double distilled water containing 20 vol% methanol as the sacrificial electron donor. Then, the sample solutions were thoroughly deaerated by bubbling nitrogen for 30 min. Next, each sample solution was irradiated by a 500 W mercury lamp (the light intensity was 0.020 W) at room temperature with continuous stirring. Finally, the evolved gases were analyzed by injecting 1 mL of headspace gas into the gas chromatograph (FULI 9750, thermal conductivity detector, nitrogen as the carrier gas, 5 Å molecular sieve column) and quantified using an external standard calibration plot.

2.5. Photoelectrochemical measurements

Photoelectrochemical performance measurements were obtained in a standard three-electrode PEC cell, with TiO₂, saturated calomel electrode and Pt wire as the working electrode, reference electrode and counter electrode, respectively. A 0.5 M Na₂SO₄ solution was used as the electrolyte and a 300 W xenon lamp was used as the light source. Electrochemical impedance spectroscopy (EIS) was performed under 300 W xenon lamp illumination at open circuit voltage over a frequency range of 0.1–100 000 Hz with a bias voltage of 0.5 V.

2.6. Characterizations of DESs and catalysts

Fourier transform infrared (FT-IR) spectra were obtained using a Varian 3100 FT-IR spectrometer. The crystal structures of the samples were detected by X-ray diffraction (XRD, Bruker D8, Germany) equipped with Cu K α radiation. Scanning electron microscopy (SEM) images were obtained on a Hitachi S4800 scanning electron microscope operating at 5.0 kV. Transmission electron microscopy (TEM) and high-resolution transmission electron microscopy (HRTEM) analyses were performed on a JEM 2010 EX instrument. Photoluminescence (PL) spectra were measured by an FLS-920 Edinburgh fluorescence spectrometer.

2.7. Method of structure optimizations

All the DFT calculations were operated using the Gaussian 03 program. The B3LYP/6-311++G (d,p) method has been used for structure optimizations. The subsequent frequency calculations at the same level verified the optimized structures to be at ground states without imaginary frequencies (NImag = 0).

3. Results and discussion

3.1. Synthesis and characterizations of DESs

Fig. 1 shows the IR spectra of ChCl, betaine, oxalic acid and the synthesized ChCl/betaine/oxalic acid DES as well as the optimized interaction structures among ChCl, betaine and oxalic acid. The vibrations of hydroxyl in ChCl showed an obvious blue shift from 3226.97 to 3393.43 cm^{-1} , while the vibrations of hydroxyl in oxalic acid and C–O⁻ in betaine simultaneously showed clear red shifts from 3421.95 to 3393.43 cm^{-1} and from 1235.29 to 1204.35 cm^{-1} . This illustrated that the H-bonds were mainly formed between hydrogen of hydroxyl in oxalic acid and Cl⁻ of ChCl as well as between hydrogen of hydroxyl in oxalic acid and O⁻ in betaine.^{10,11} DFT calculations displayed that the energy minimum structure of this DES was really formed by H-bonds between hydrogen of hydroxyl in oxalic acid and Cl⁻ of ChCl as well as between hydrogen of hydroxyl in oxalic acid and O⁻ in betaine. Just the formation of these H-bonds led to the corresponding bond length changes. The bond lengths of hydroxyl in ChCl became shorter from 0.989 to 0.979 Å, while the bond lengths of hydroxyl in oxalic acid and C–O⁻ in betaine

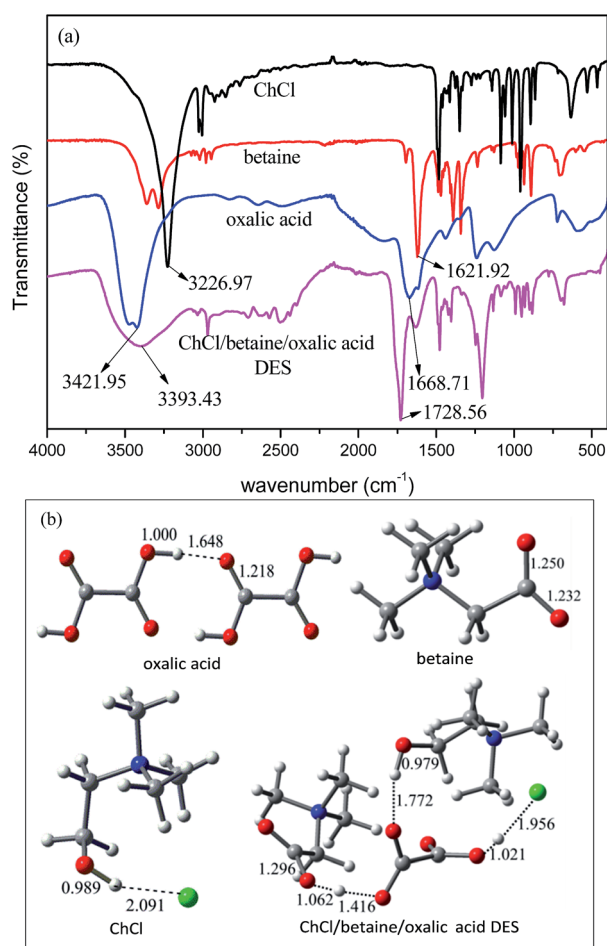


Fig. 1 (a) IR spectra of the synthesized ChCl/betaine/oxalic acid DES, ChCl, betaine and oxalic acid, and (b) optimized interaction structures among ChCl, betaine and oxalic acid by B3LYP/6-311++G(d,p). Red: O; green: Cl; blue: N; white: H; dark grey: C.

became longer from 1.000 to 1.021 (and 1.416) Å and from 1.232 (and 1.250) to 1.296 Å. The change trends were consistent with the FT-IR results.

3.2. Synthesis and characterization of heterophase-junction TiO₂

The XRD patterns of all TiO₂ samples prepared with different molar ratios of ChCl to betaine are shown in Fig. 2. The major diffraction peaks at 25.39°, 30.67° and 48.12° can be assigned to the (120), (121) and (231) facets of brookite TiO₂ (JCPDS 29-1360), respectively. Furthermore, the peaks at 27.34°, 36.09°, 41.18°, 54.10° and 69.71° are ascribed to the (110), (101), (111), (211) and (112) facets of rutile TiO₂ (JCPDS 21-1276), respectively; however, some of the characteristic peaks of anatase (such as 75.12°) are absent.^{6a,12} These results demonstrate that the prepared TiO₂ with DES only contained both brookite phase and rutile phase. In addition, it could be observed that the characteristic peak intensities of two phases at 25.39° and 27.34° changed with the molar ratios of ChCl to betaine. The peak intensity of the brookite phase at 25.39° gradually increased, while the peak intensity of rutile gradually decreased simultaneously with the increase in the molar ratios of ChCl to betaine. This illustrated that the brookite phase content gradually increased as the molar ratios of ChCl to betaine increased. Thus, it can be seen that ChCl in DES tends to form the brookite phase, betaine tends to form the rutile phase, and the ratios of the two phases can be easily adjusted by changing the ratios of the two H-bond acceptors.

The morphologies of the TiO₂ samples synthesized with DES ChCl/betaine/oxalic acid with different molar ratios of ChCl to betaine were determined; the results are shown in Fig. 3. When the molar ratio of ChCl to betaine was 1 : 6, microspheres were formed by the assembly of needle-like nanoparticles. When the molar ratios of ChCl to betaine were between 1 : 3 and 1 : 1, needle-like microspheres with needle-like clusters were obtained. When the molar ratio of ChCl to betaine was 2 : 1, microspheres with a uniform size and good dispersion were

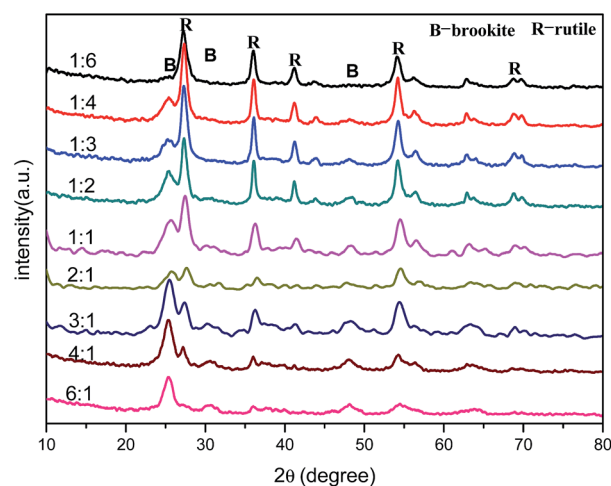


Fig. 2 XRD patterns of TiO₂ samples prepared with different molar ratios of ChCl to betaine.

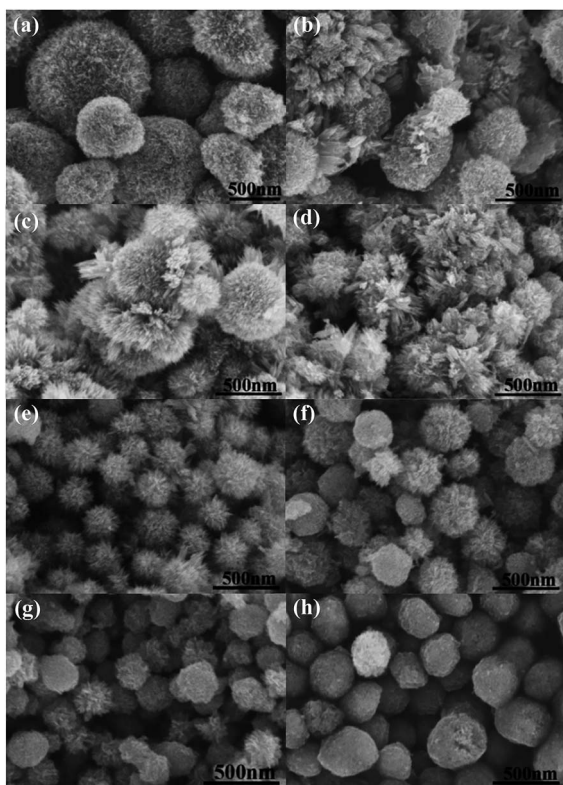


Fig. 3 SEM images of TiO_2 samples prepared with different molar ratios of ChCl to betaine: (a) 1 : 6, (b) 1 : 3, (c) 1 : 2, (d) 1 : 1, (e) 2 : 1, (f) 3 : 1, (g) 4 : 1 and (h) 6 : 1.

formed by thin needle-like nanoparticles. When the molar ratios of ChCl to betaine were between 3 : 1 and 6 : 1, the shapes gradually shifted from the needle-like microspheres to relatively tight and smooth-surfaced microspheres. These results illustrate that rutile tended to present loosely needle-like microspheres, while brookite tended to present tight and smooth-surfaced nanoparticles.

The TEM images in Fig. 4(a) and (b) also reveal that the phase-junction TiO_2 synthesized at 2 : 1 molar ratio of ChCl to betaine comprises microspheres constructed by thin needle-like nanoparticles. Fig. 4(c) shows an HRTEM image. The lattice fringes with spacings of 0.3 nm and 0.219 nm correspond to the d -spacings of the (201) and (111) planes of brookite phase TiO_2 , while the lattice fringes with the spacing of 0.319 nm correspond to the d -spacing of the (110) planes of rutile phase TiO_2 , which confirmed that both brookite phase and rutile phase existed in TiO_2 synthesized by this method. Moreover, the shapes of TiO_2 synthesized at 2 : 1 molar ratio of ChCl to betaine were regular, which illustrated that both brookite phase and rutile phase coexisted in the same nanoparticle. Therefore, HRTEM, TEM, SEM and XRD together proved that the brookite-rutile phase-junction TiO_2 was successfully prepared. In addition, Fig. 4(c) clearly shows some lattice dislocations and disorder, which suggest a defect structure.¹³ These defects may benefit the exposure of more active sites and the enhancement of light absorption.¹³ These results indicate a new, green, mild

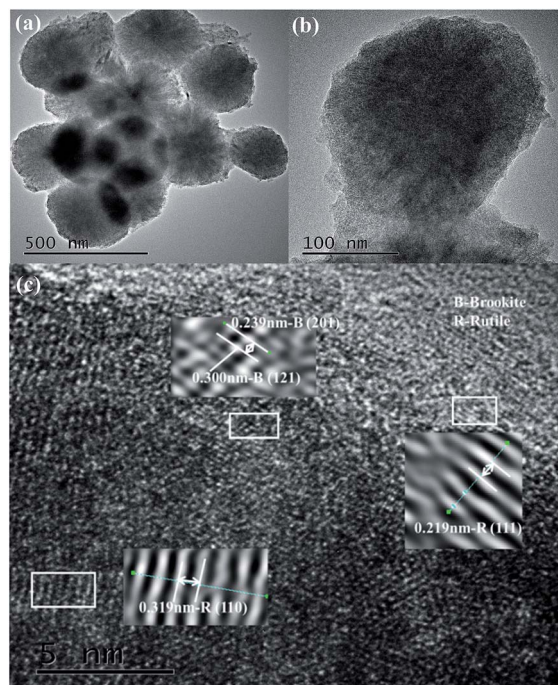


Fig. 4 (a and b) TEM and (c) HRTEM images of TiO_2 synthesized at 2 : 1 molar ratio of ChCl to betaine.

and versatile preparation method of heterophase-junction nano-catalysts.

3.3 Test of catalytic activity

The photocatalytic activities of the synthesized phase-junction TiO_2 with different molar ratios of ChCl to betaine were evaluated in comparison with that of commercial P25 TiO_2 and the results are shown in Fig. 5(a). It can be seen that phase-junction TiO_2 shows much higher photocatalytic activities than commercial P25 TiO_2 . Especially, when the molar ratio of ChCl to betaine is 2 : 1, the H_2 production rate from photocatalytic water splitting reaches up to $14.51 \text{ mmol h}^{-1} \text{ g}^{-1}$, which is 20-fold greater than that of commercial P25 TiO_2 . Obviously, the phase percentage in the phase-junction TiO_2 can be regulated more easily under mild reaction conditions in this method; moreover, the activity is much higher than that of the other reported TiO_2 and even higher than that of some noble metal-doped TiO_2 compounds.¹⁴ To test the stability of phase-junction TiO_2 , a recycling experiment of the H_2 evolution rate of the TiO_2 sample with 2 : 1 molar ratio of ChCl to betaine was carried out. As shown in Fig. 5(b), no obvious H_2 evolution rate decrease is observed within five cycles in 30 h, which demonstrates the photostability of phase-junction TiO_2 prepared by this method.

3.4 Photoelectrochemical properties

PL emission is mainly caused by the recombination of excited electrons and holes; thus, it is considered as an effective way for understanding the separation capacity of the photo-induced carriers. A low PL intensity usually indicates decrease in the

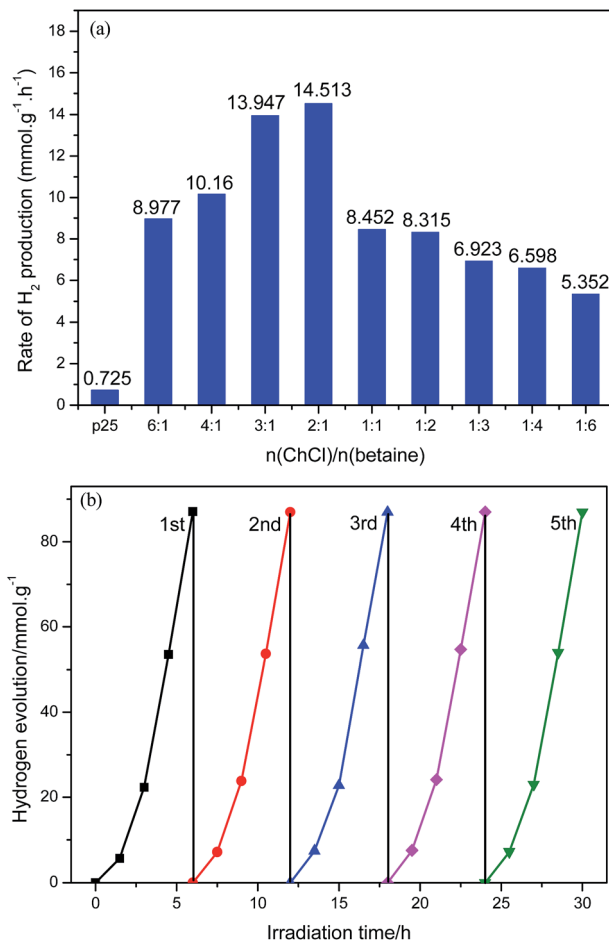


Fig. 5 (a) H₂ evolution rate of commercial P25 TiO₂ and phase-junction TiO₂ with different molar ratios of ChCl to betaine; (b) cyclic runs for the photocatalytic H₂ production of TiO₂ sample with 2 : 1 molar ratio of ChCl to betaine.

recombination rate.¹⁵ Fig. 6 presents a comparison of the PL spectra of the samples and commercial P25 TiO₂ in a wavelength range of 380–600 nm. It can be seen that the main peaks

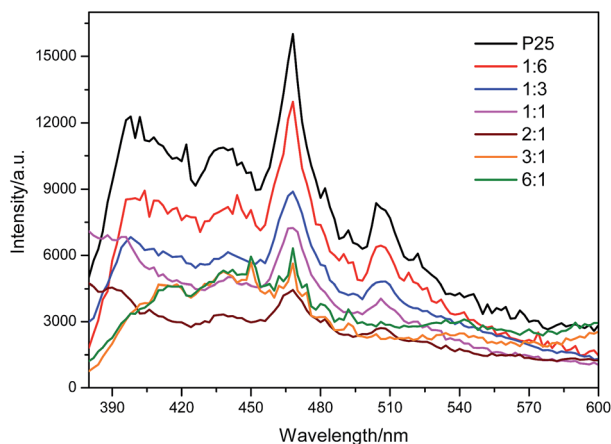


Fig. 6 PL spectra of the synthesized phase-junction TiO₂ photocatalysts with different molar ratios of ChCl to betaine and commercial P25 TiO₂ (excitation wavelength: 315 nm).

display similar shapes; the PL intensities of the TiO₂ samples are far lower than that of commercial P25 TiO₂ and that of the TiO₂ sample synthesized at 2 : 1 molar ratio of ChCl to betaine is the weakest. The PL measurement results were consistent with the order of the photocatalytic activities. These findings indicated that phase-junction TiO₂ prepared by this method has a relatively low electron and hole recombination rate.

Photocurrent measurements were obtained for the phase-junction TiO₂ with different molar ratios of ChCl to betaine as well as for commercial P25 TiO₂; the results are shown in Fig. 7. The photocurrent responses of the TiO₂ samples were far higher than that of commercial P25 TiO₂ and that of the TiO₂ sample synthesized at 2 : 1 molar ratio of ChCl to betaine was the highest; this was consistent with the order of the photocatalytic activities. These results indicated that the phase-junction TiO₂ samples have improved charge separation and migration efficiency.¹⁶

EIS was also performed for commercial P25 TiO₂ and phase-junction TiO₂ with different molar ratios of ChCl to betaine after full spectrum irradiation. As presented in Fig. 8, the diameters of the arc radius on the EIS Nyquist plot of the synthesized TiO₂ samples are all smaller than that of the commercial P25 TiO₂ electrode, and that of the TiO₂ sample synthesized at 2 : 1 molar ratio of ChCl to betaine is the smallest. The smaller the arc radius of an EIS Nyquist plot, the higher the efficiency of charge separation.^{16,17} Thus, in the case of phase-junction TiO₂, the photoinduced electron–hole pairs were easily separated and transferred to the sample surface.

The results of PL spectra, photocurrent responses and EIS revealed that the improvement in the photocatalytic activity of phase-junction TiO₂ may benefit from the improvements in electron–hole separation efficiency, charge transfer rates and the suppression of electron–hole pair recombination due to the existence of a phase junction.

3.5 Effect of defects on the catalytic activity

To further understand the cause of the high activity of phase-junction TiO₂, we repaired the surface defects of the

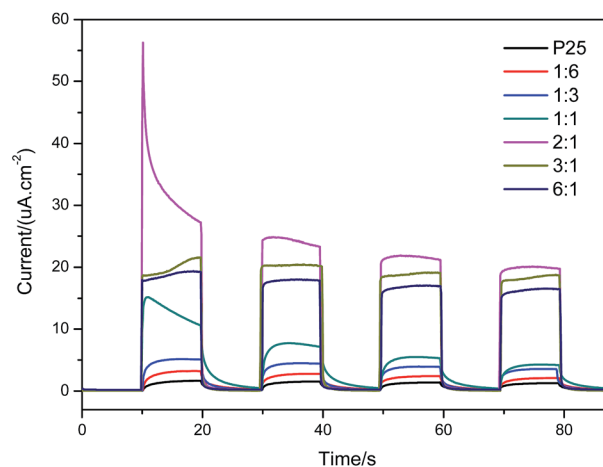


Fig. 7 Photocurrent responses of phase-junction TiO₂ with different molar ratios of ChCl to betaine and commercial P25 TiO₂.

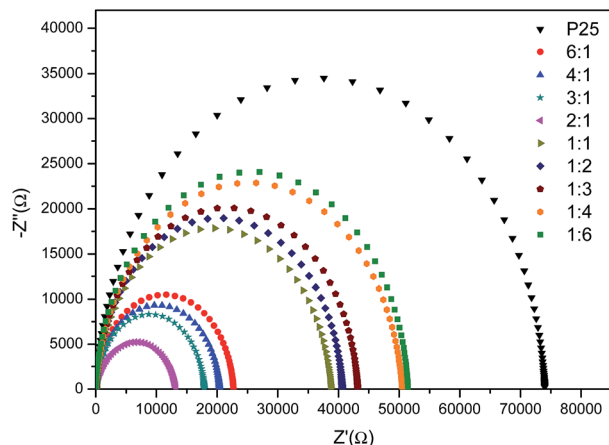


Fig. 8 EIS of commercial P25 TiO_2 and phase-junction TiO_2 with different molar ratios of ChCl to betaine after irradiation.

synthesized TiO_2 with 1 : 6 molar ratio of ChCl to betaine by the slow programmed heating and programmed cooling method. Then, we compared the XRD patterns, HRTEM images and the photocatalytic activities before and after repairing the defects. The XRD patterns and HRTEM images before and after repairing defects are shown in Fig. 9. The XRD patterns show that the position and relative strength of the characteristic peaks of the samples before and after repairing defects are consistent, which illustrate that the crystalline phase did not change. The HRTEM image displays that the lattice dislocations and disorder almost disappear after repairing defects. Moreover, the photocatalytic activity after repairing defects is $3.22 \text{ mmol h}^{-1} \text{ g}^{-1}$, which is obviously lower than $5.35 \text{ mmol h}^{-1} \text{ g}^{-1}$ before repairing defects. This illustrates that the defects resulting from the lattice disorder can be another important reason for the improvement in the photocatalytic activity. To further verify the effect of defects on activity, we also compared the samples before and after repairing defects using TiO_2 synthesized at 2 : 1

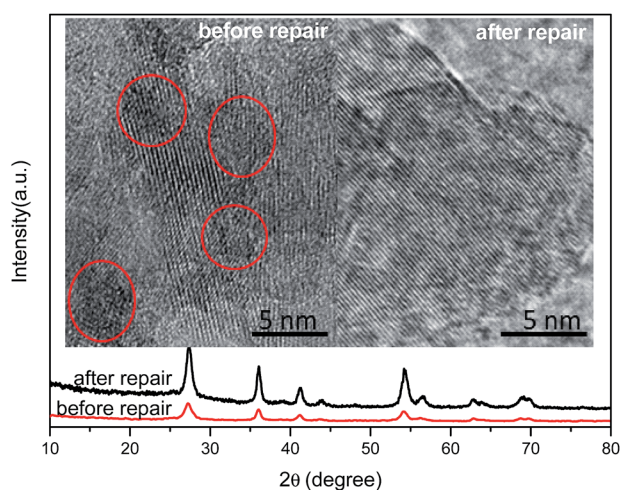


Fig. 9 Comparison of XRD patterns and HRTEM images before and after repairing defects.

molar ratio of ChCl to betaine; the results are consistent with our conclusion mentioned above (Fig. S1†).

Therefore, the high activity of the TiO_2 samples prepared by this method mainly resulted from the combined effect of both phase junctions and surface defects caused by lattice dislocations and disorder. These results indicate a promising industrial prospect in the nanomaterial preparation due to the following aspects: DESs that are green, low-cost, and easy to prepare on a large scale; a mild, clean and facile material preparation process; and a stable and efficient nanocatalyst.

4. Conclusions

Aiming to solve the problems of high-temperature calcination, long preparation time, tedious synthetic procedure, and complicated synthesis system, ChCl/betaine/oxalic acid DES was prepared and used for the controllable synthesis of heterophase-junction nano- TiO_2 with different phase ratios under green and mild reaction conditions (at 180°C for 18 h); here, ChCl/betaine/oxalic acid DES was used as the solvent, template, inhibitor and crystalline phase control agent at the same time. The H_2 production rate in the photocatalytic water splitting of this heterophase-junction nano- TiO_2 reached up to $14.51 \text{ mmol h}^{-1} \text{ g}^{-1}$, which was 20-fold greater than that of commercial P25 TiO_2 ; till date, this is the highest value for water splitting into hydrogen catalyzed by sole TiO_2 . These higher photocatalytic activities of the TiO_2 samples were attributed to the phase junctions and defects caused by lattice dislocations and disorder. This study will provide a new method for the green, mild and easily controllable preparation of heterophase-junction catalysts with high efficiency as well as a new way for the batch preparation of nano-catalysts at the same time.

Conflicts of interest

There are no conflicts to declare.

Acknowledgements

This work was supported by the National Natural Science Foundation of China (21535004, 91753111, 21808129, 21405096), the Key Research and Development Program of Shandong Provincial (2018YFJH0502) and Shandong Provincial Natural Science Foundation, China (ZR2014BQ018).

Notes and references

- (a) M. Z. Ge, J. S. Cai, J. Iocozzia, C. Y. Cao, J. Y. Huang, X. N. Zhang, J. L. Shen, S. C. Wang, S. N. Zhang, K. Q. Zhang, Y. K. Lai and Z. Q. Lin, *Int. J. Hydrogen Energy*, 2017, **42**, 8418; (b) H. T. T. Tran, H. Kosslick, M. F. Ibad, C. Fischer, U. Bentrup, T. H. Vuong, L. Q. Nguyen and A. Schulz, *Appl. Catal., B*, 2017, **200**, 647; (c) R. G. Li, Y. X. Weng, X. Zhou, X. L. Wang, Y. Mi, R. F. Chong, H. X. Han and C. Li, *Energy Environ. Sci.*, 2015, **8**, 2377; (d) W. J. Yin, B. Wen, C. Y. Zhou, A. Selloni and L. M. Liu, *Surf. Sci. Rep.*, 2018, **73**, 58.

- 2 S. Bakardjieva, J. Subrt, V. Stengla, M. J. Dianez and M. J. Sayagues, *Appl. Catal., B*, 2005, **58**, 193.
- 3 (a) Y. L. Wang, W. Zhang, Z. H. Wang, Y. M. Cao, J. M. Feng, Z. L. Wang and Y. Ma, *Chin. J. Catal.*, 2018, **39**, 1500; (b) W. K. Wang, J. J. Chen, X. Zhang, Y. X. Huang, W. W. Li and H. Q. Yu, *Sci. Rep.*, 2016, **6**, 20491; (c) A. L. Li, Z. L. Wang, H. Yin, S. Y. Wang, P. L. Yan, B. K. Huang, X. L. Wang, R. G. Li, X. Zong, H. X. Han and C. Li, *Chem. Sci.*, 2016, **7**, 6076.
- 4 Z. Ambrus, K. Mogyorosi, A. Szalai, T. Alapi, K. Demeter, A. Dombi and P. Sipos, *Appl. Catal., A*, 2008, **340**, 153.
- 5 (a) T. A. Kandiel, A. Feldhoff, L. Robben, R. Dillert and D. W. Bahnemann, *Chem. Mater.*, 2010, **22**, 2050; (b) S. M. El-Sheikh, T. M. Khedr, G. S. Zhang, V. Vogiazzi, A. A. Ismail, K. O'Shea and D. D. Dionysiou, *Chem. Eng. J.*, 2017, **310**, 428; (c) J. A. Diaz-Real, J. W. Maa and N. Alonso-Vante, *Appl. Catal., B*, 2016, **198**, 471.
- 6 (a) O. Pikuda, C. Garlisi, G. Scandura and G. Palmisano, *J. Catal.*, 2017, **346**, 109; (b) Y. F. Cao, X. T. Li, Z. F. Bian, A. Fuhr, D. Q. Zhang and J. Zhu, *Appl. Catal., B*, 2016, **180**, 551.
- 7 (a) R. Kaplan, B. Erjavec, G. Drazic, J. Grdadolnik and A. Pintar, *Appl. Catal., B*, 2016, **181**, 465; (b) Y. L. Liao, W. X. Que, Q. Y. Jia, Y. C. He, J. Zhang and P. Zhong, *J. Mater. Chem.*, 2012, **22**, 7937.
- 8 (a) D. V. Wagle, H. Zhao and G. A. Baker, *Acc. Chem. Res.*, 2014, **47**, 2299; (b) R. P. Xin, S. J. Qi, C. X. Zeng, F. I. Khan, B. Yang and Y. H. Wang, *Food Chem.*, 2017, **217**, 560.
- 9 M. C. Gutierrez, D. Carriazo, A. Tamayo, R. Jimenez, F. Pico, J. M. Rojo, M. L. Ferrer and F. del Monte, *Chem.-Eur. J.*, 2011, **17**, 10533.
- 10 Q. Wang, B. H. Dong, Y. Q. Zhao, F. Huang, J. F. Xie, G. W. Cui and B. Tang, *Chem. Eng. J.*, 2018, **46**, 811.
- 11 M. Francisco, A. van den Bruinhorst and M. C. Kroon, *Angew. Chem., Int. Ed.*, 2013, **52**, 3074.
- 12 T. Balaganapathi, B. Kaniyathasan, S. Vinoth, T. Arun and P. Thilakan, *Ceram. Int.*, 2017, **43**, 2438.
- 13 (a) J. F. Xie, H. Zhang, S. Li, R. X. Wang, X. Sun, M. Zhou, J. F. Zhou, X. W. Lou and Y. Xie, *Adv. Mater.*, 2013, **25**, 5807; (b) J. F. Xie, C. Z. Wu, S. L. Hu, J. Dai, N. Zhang, J. Feng, J. L. Yang and Y. Xie, *Phys. Chem. Chem. Phys.*, 2012, **14**, 4810; (c) Q. Cao, Y. F. Cheng, H. Bi, X. B. Zhao, K. P. Yuan, Q. H. Liu, Q. Q. Li, M. Wang and R. C. Che, *J. Mater. Chem. A*, 2015, **3**, 20051; (d) Y. Y. Zhu, Q. Ling, Y. F. Liu, H. Wang and Y. F. Zhu, *Appl. Catal., B*, 2016, **187**, 204; (e) C. Haw, W. Chiu, S. A. Rahman, P. Khiew, S. Radiman, R. A. Shukor, M. A. A. Hamid and N. Ghazali, *New J. Chem.*, 2016, **40**, 1124.
- 14 (a) W. T. Chen, A. Chan, Z. H. N. Al-Azri, A. G. Dosado, M. A. Nadeem, D. X. Sun-Waterhouse, H. Idriss and G. I. N. Waterhouse, *J. Catal.*, 2015, **329**, 499; (b) Y. L. Sui, S. B. Liu, T. F. Li, Q. X. Liu, T. Jiang, Y. F. Guo and J. L. Luo, *J. Catal.*, 2017, **353**, 250; (c) Y. H. Cao, Q. Y. Li, C. Li, J. L. Li and J. J. Yang, *Appl. Catal., B*, 2016, **198**, 378.
- 15 X. L. Weng, Q. S. Zeng, Y. L. Zhang, F. Dong and Z. B. Wu, *ACS Sustainable Chem. Eng.*, 2016, **4**, 4314.
- 16 Q. Wang, J. Y. Huang, H. T. Sun, K. Q. Zhang and Y. K. Lai, *Nanoscale*, 2017, **9**, 16046.
- 17 M. W. Kim, K. Kim, T. Y. Ohm, H. Yoon, B. Joshi, E. Samuel, M. T. Swihart, S. K. Choi, H. Park and S. S. Yoon, *Chem. Eng. J.*, 2018, **333**, 721.